Iterative Joint Channel Estimation and Multiuser Detection for Wireless MIMO-OFDM Systems: Performance in a Real Indoor Scenario

Pierluigi Salvo Rossi [#], Parisa Pakniat [*], Ralf R. Müller [#], Ove Edfors [*]

[#]*Department of Electronic and Telecommunications, Norwegian University of Science and Technology*
O.S. Bragstads plass 2B, 7491 Trondheim, Norway
{salvoros,mueller}@iet.ntnu.no

[*]*Department of Elecroscience, Lund University*
Ole Römers väg 3, 22100 Lund, Sweden
{Parisa.Pakniat,Ove.Edfors}@es.lth.se

***Abstract*— An iterative receiver for Multiple-Input Multiple-Output (MIMO) Orthogonal Frequency Division Multiplexing (OFDM) wireless systems is presented and tested on channel measurements from a real indoor scenario. The receiver jointly performs channel estimation and multiuser detection, with soft information iteratively provided by the singleuser decoders. Results for the performance are presented in terms of Bit Error Rate (BER) and relative Minimum Mean Square Error (MMSE) vs Signal-to-Noise Ratio (SNR). Comparison with the Single-User Bound (SUB) shows a loss in performance due to frequency correlation.**

I. Introduction

High-data-rate wireless communication with quality of service comparable to wireline technologies is a strong need of the modern society of information, due to the increasing demand of multimedia services for mobile users. Multiple antennas at both transmit and receiver side, providing a Multiple-Input Multiple-Output (MIMO) channel, represent an attractive solution to obtain either a diversity gain or a capacity gain [4]. As for the latter, increasing capacity by a factor of the minimum number of transmit and receive antennas is very suited to future-services requirements. Orthogonal Frequency Division Multiplexing (OFDM) has been adopted in several standards [4] providing high data rates. OFDM requires simple channel equalization via conversion of a frequency-selective channel into a set of frequency-flat subchannels. MIMO-OFDM systems for wireless high-data-rate communications have been studied to mitigate inter-symbol interference and enhance system capacity at the same time [6], [13].

Iterative receivers [3], [16] for multiuser detection [15] represent the key technology for next-generation systems as they achieve excellent performance with contained complexity and confirmed attractive also for MIMO-OFDM systems [5], [7], [9]. Iterative joint multiuser detection and channel estimation have been also studied in various scenario [8], [12], [17].

[0]This work has been supported by the Research Council of Norway (RCN) and by the Swedish Governmental Agency for Innovations Systems (VINNOVA) under WILATI project within the NORDITE research program.

This paper describes the performance of an iterative receiver for MIMO-OFDM systems performing joint channel estimation and multiuser detection [12] on a real indoor scenario with people walking and interferer devices. The main contribution is that shown results reflect what a user would really experience in an indoor scenario. It is organized as follows: the mathematical model for the considered MIMO-OFDM system is described in Sec. II; Sec. III describes the structure of the iterative receiver; the real scenario on which the receiver is tested is described in Sec. IV; Sec V shows the performance in terms of Bit Error Rate (BER) and relative Minimum Mean Square Error (MMSE) with respect to Signal-to-Noise Ratio (SNR); some conclusions are given in Sec. VI.

Notation - Column vectors (resp. matrices) are denoted with lower-case (resp. upper-case) bold letters; a_i (resp. $A_{i,j}$) denotes the ith (resp. (i,j)th) element of vector $\boldsymbol{a}$ (resp. matrix $\boldsymbol{A}$); $\mathrm{diag}(\boldsymbol{a})$ denotes a diagonal matrix whose main diagonal is $\boldsymbol{a}$. $\boldsymbol{I}_N$ denotes the $N \times N$ identity matrix; $\boldsymbol{i}_N^{(n)}$ denotes the nth column of $\boldsymbol{I}_N$; $\boldsymbol{e}_N$ (resp. $\boldsymbol{o}_N$) denotes a vector of length N whose elements are 1 (resp. 0); $\mathbb{E}\{.\}$, $(.)^*$, $(.)^{\mathrm{T}}$ and $(.)^{\mathrm{H}}$ denote expectation, conjugate, transpose and conjugate transpose operators; $\delta_{n,m}$ denotes the Kronecker delta; $\otimes$ denotes the Kronecker matrix product; $\lceil a \rceil$ denotes the smallest integer value greater or equal than a; $\sim \mathcal{N}_{\mathbb{C}}(\boldsymbol{\mu}, \boldsymbol{\Sigma})$ means "distributed according to a circular symmetric complex normal distribution with mean $\boldsymbol{\mu}$ and covariance $\boldsymbol{\Sigma}$".

II. System Model

We consider a MIMO-OFDM system with K transmit antennas, N receive antennas, M subcarriers, and assume that each transmit antenna sends an independent data stream. The bit stream is divided in blocks of L_b source bits; each block is encoded via a convolutional encoder and a random interleaver [10]; L_p pilot bits are inserted to produce a frame of L code bits. The bits of the frame are mapped into symbols via Binary Phase Shift Keying (BPSK) modulation [10]. The symbols are grouped into $S = L/M$ blocks, and each block gives rise to an OFDM symbol to be transmitted on the wireless channel.

The S OFDM symbols from the same frame are called OFDM block. We assume that both L and L_p are integer multiples of M, thus we have $S_p = L_p/M$ pilot OFDM symbols and $S-S_p$ data OFDM symbols. Optimal pilot placement falls beyond the scope of this paper, and we simply assume that pilot OFDM symbols are distributed in the OFDM block according to the set of indexes $\left\{ \left\lceil \frac{(2s-1)S}{2S_p} \right\rceil \right\}_{s=1}^{S_p}$.

In the following: $b_k[\ell]$ and $c_k[\ell]$ respectively denote the ℓth source bit and the ℓth code bit (including pilots) to be transmitted by the kth transmit antenna; during transmission of the sth OFDM symbol, on the mth subcarrier, $x_k[m,s]$, $H_{n,k}[m,s]$, $w_n[m,s]$, $r_n[m,s]$ denote the (*Frequency Domain*) symbol transmitted by the kth transmit antenna, the (*Frequency Domain*) channel coefficient between the kth transmit antenna and the nth receive antenna, the (*Frequency Domain*) additive noise at the nth receive antenna, the (*Frequency Domain*) received signal at the nth receive antenna, respectively.

We denote the transmitted vector, the channel matrix, the noise vector ($\sim \mathcal{N}_{\mathbb{C}}(\boldsymbol{o}, \sigma_w^2 \boldsymbol{I}_N)$), and the received vector as

$$\begin{aligned} \boldsymbol{x}[m,s] &= (x_1[m,s], \ldots, x_K[m,s])^{\mathrm{T}} , \\ \boldsymbol{H}[m,s] &= \begin{pmatrix} H_{1,1}[m,s] & \ldots & H_{1,K}[m,s] \\ \vdots & \ddots & \vdots \\ H_{N,1}[m,s] & \ldots & H_{N,K}[m,s] \end{pmatrix} , \\ \boldsymbol{w}[m,s] &= (w_1[m,s], \ldots, w_N[m,s])^{\mathrm{T}} , \\ \boldsymbol{r}[m,s] &= (r_1[m,s], \ldots, r_N[m,s])^{\mathrm{T}} , \end{aligned}$$

and assume that the length of the cyclic prefix (L_{cp}) exceeds the channel delay spread, then the discrete-time model for the received signal is

$$\boldsymbol{r}[m,s] = \boldsymbol{H}[m,s]\boldsymbol{x}[m,s] + \boldsymbol{w}[m,s] . \tag{1}$$

We denote the channel vector from kth transmit antenna as $\boldsymbol{h}_{(k)}[m,s] = \boldsymbol{H}[m,s]\boldsymbol{i}_K^{(k)}$. It is worth noticing that m and s represent frequency-variation and time-variation, respectively.

III. The Receiver

Transmissions from the various antennas combine at each receive antenna and are processed according to the following receiver. We ignore time asynchrony among transmit antennas, reasonable if synchronization errors do not exceed the length of the cyclic prefix. Referring to the generic OFDM block, the receiver iteratively performs: multiuser detection, singleuser decoding, channel estimation.

Both multiuser detector and singleuser decoders exchange extrinsic-based soft information on symbols x_k. We denote $\tilde{x_k}$ the one passing from the singleuser decoders to the multiuser detector, and $\tilde{z_k}$ the one passing in the opposite way. singleuser decoders also provide *a posteriori*-based soft information on symbol x_k, denoted $\hat{x_k}$, to the channel estimator, and *a posteriori*-based soft information on source bit, denoted d_k. The channel estimator provides channel coefficient estimates to the multiuser detector, denoted $\hat{H}_{n,k}$. It is worth noticing that $\{\tilde{z_k}[1], \ldots, \tilde{z_k}[L]\}$ are deinterleaved before being passed to the the SISO decoder, while $\{\tilde{x_k}[1], \ldots, \tilde{x_k}[L]\}$ and $\{\hat{x_k}[1], \ldots, \hat{x_k}[L]\}$ are interleaved before being passed to the MUD and to the channel estimator, respectively. In the following we do NOT introduce different notations in order to explicitly distinguish interleaved and deinterleaved symbols, and leave the meaning to be evinced from the context.

A. Multiuser detection

Multiuser detection is performed via parallel interference cancellation and MMSE filtering. More precisely, the received signals (1) are processed separately for each subcarrier and for each OFDM symbol. We omit the indexes m and s to simplify notation. In the derivation of the symbol extrinsic soft information, we assume that the receiver has perfect knowledge of the channel coefficients, while in practice estimates from the channel estimator are used ($\boldsymbol{H}$ is replaced with $\hat{\boldsymbol{H}}$).

The detector receives $\tilde{\boldsymbol{x}}$ from the singleuser decoders and $\boldsymbol{H}$ from the channel estimators. Denoting $\tilde{\boldsymbol{x}}_{(k)} = \tilde{\boldsymbol{x}} - \tilde{x}_k \boldsymbol{i}_K^{(k)}$, for each transmit antenna it is possible to compute the residual term from the interference cancellation as

$$\tilde{\boldsymbol{r}}_{(k)} = \boldsymbol{r} - \boldsymbol{H}\tilde{\boldsymbol{x}}_{(k)} . \tag{2}$$

The residual term is then processed with an MMSE filter, in order to reduce further the effects of noise and MAI, giving the extrinsic-based soft information

$$\tilde{z}_k = \boldsymbol{f}_{(k)}^{\mathrm{H}} \tilde{\boldsymbol{r}}_{(k)} .$$

The filter is found as $\boldsymbol{f}_{(k)} = \arg\min_{\boldsymbol{f}} \mathbb{E}\left\{|x_k - \boldsymbol{f}^{\mathrm{H}}\tilde{\boldsymbol{r}}_{(k)}|^2\right\}$ $= \left(\mathbb{E}\left\{\tilde{\boldsymbol{r}}_{(k)}\tilde{\boldsymbol{r}}_{(k)}^{\mathrm{H}}\right\}\right)^{-1} \mathbb{E}\left\{x_k \tilde{\boldsymbol{r}}_{(k)}\right\}$. From (1) and (2) we have

$$\begin{aligned} \mathbb{E}\left\{\tilde{\boldsymbol{r}}_{(k)}\tilde{\boldsymbol{r}}_{(k)}^{\mathrm{H}}\right\} &= \boldsymbol{H}\boldsymbol{V}_{(k)}\boldsymbol{H}^{\mathrm{H}} + \sigma_w^2 \boldsymbol{I}_N , \\ \mathbb{E}\left\{x_k \tilde{\boldsymbol{r}}_{(k)}\right\} &= \boldsymbol{h}_{(k)} , \end{aligned}$$

being $\boldsymbol{V}_{(k)} = \mathrm{diag}\left((1-|\tilde{x}_1|^2, \ldots, 1-|\tilde{x}_{k-1}|^2, 1, 1-|\tilde{x}_{k+1}|^2, \ldots, 1-|\tilde{x}_K|^2)\right)$, thus giving

$$\tilde{z}_k = \boldsymbol{h}_{(k)}^{\mathrm{H}} \left(\boldsymbol{H}\boldsymbol{V}_{(k)}\boldsymbol{H}^{\mathrm{H}} + \sigma_w^2 \boldsymbol{I}_N\right)^{-1} \tilde{\boldsymbol{r}}_{(k)} .$$

The unbiased estimate is then

$$\tilde{z}_k = \frac{\boldsymbol{h}_{(k)}^{\mathrm{H}} \left(\boldsymbol{H}\boldsymbol{V}_{(k)}\boldsymbol{H}^{\mathrm{H}} + \sigma_w^2 \boldsymbol{I}_N\right)^{-1} \tilde{\boldsymbol{r}}_{(k)}}{\boldsymbol{h}_{(k)}^{\mathrm{H}} \left(\boldsymbol{H}\boldsymbol{V}_{(k)}\boldsymbol{H}^{\mathrm{H}} + \sigma_w^2 \boldsymbol{I}_N\right)^{-1} \boldsymbol{h}_{(k)}} .$$

B. Singleuser Decoding

After collecting $\{z_k[1], \ldots, z_k[L]\}$, each transmit antenna can be decoded independently using the BCJR algorithm [2]. It is worth noticing that $z_k[\ell]$ has been transmitted on the mth subcarrier during the sth OFDM symbol if $\ell = (s-1)M + m$. The model for the output of the MUD [16], used by the decoder for the kth transmit antenna, is $z_k = \mu_k x_k + v_k$, with $v_k \sim \mathcal{N}_{\mathbb{C}}(0, \eta_k^2)$, where $\mu_k = 1$, and $\eta_k^2 = \left(\boldsymbol{h}_{(k)}^{\mathrm{H}} \left(\boldsymbol{H}\boldsymbol{V}_{(k)}\boldsymbol{H}^{\mathrm{H}} + \sigma_w^2 \boldsymbol{I}_N\right)^{-1} \boldsymbol{h}_{(k)}\right)^{-1}$. We omit the index k to simplify notation.

Using a trellis representation for the code, let $\varsigma_t \in \{1, \ldots, Q\}$ be the state of the trellis at the end of the tth transition among T total transitions. The tth transition

corresponds to the tth group of source bits entering the encoder [10]. Forward and backward variables are computed according to the following recursions:

$$\alpha_t(j) = \sum_{i=1}^{Q} \alpha_{t-1}(i)\gamma_t(i,j) \ , \ \beta_t(i) = \sum_{j=1}^{Q} \gamma_{t+1}(i,j)\beta_{t+1}(j) \ ,$$

where the initialization is given by $\alpha_0(i) = \delta_{i,1}$ and $\beta_T(j) = \delta_{j,1}$, and where $\gamma_t(i,j) = \Pr(\varsigma_t = j|\varsigma_{t-1} = i) \times \prod_{o=1}^{n_0} \Pr\left(z[(t-1)n_0+o]|x_{i\to j}[(t-1)n_0+o]\right)$, being $x_{i\to j}[(t-1)n_0+o]$ the oth symbol among the n_0 that would have been transmitted during the tth transition with $\varsigma_{t-1} = i$ and $\varsigma_t = j$. The initialization of the forward and backward variables takes into account the fact that the encoder starts in state 1 and, due to the insertion of appropriate tail bits to the block of source bits within the frame, also stops in state 1.

The *a posteriori* likelihood and the extrinsic likelihood are obtained respectively as

$$\Lambda_{\mathrm{APP}}(x[\ell]|z[1],\ldots,z[L]) = \frac{\sum_{(i,j):x[\ell]=+1} \alpha_{t-1}(i)\gamma_t(i,j)\beta_t(j)}{\sum_{(i,j):x[\ell]=-1} \alpha_{t-1}(i)\gamma_t(i,j)\beta_t(j)}$$

$$\Lambda_{\mathrm{EXT}}(x[\ell]|z[1],\ldots,z[L]) = \frac{\Lambda_{\mathrm{APP}}(x[\ell]|z[1],\ldots,z[L])}{\frac{\Pr(z[\ell]|x[\ell]=+1)}{\Pr(z[\ell]|x[\ell]=-1)}} \ ,$$

being $\Pr(z|x) = \frac{1}{\sqrt{2\pi\eta^2}} \exp\left(-\frac{|z-\mu x|^2}{2\eta^2}\right)$. More specifically, the algorithm is implemented in the log-domain [11].

C. Channel Estimation

For channel estimation we use a Slepian basis expansion of the channel coefficient, that shown to be very effective for time variant channels [17],

$$\hat{H}_{n,k}(m,s) \approx \sum_{i=1}^{I} \psi_{n,k}[m,i]u_i[s] \ , \tag{3}$$

where $u_i[s]$ is the sth sample of the ith discrete prolate spheroidal sequence defined as the solution to

$$\sum_{s'=1}^{S} 2\nu_{\max}^{(\mathrm{D})}\mathrm{sinc}\left(2\nu_{\max}^{(\mathrm{D})}(s'-s)\right)u_i[s'] = \lambda_i(\nu_{\max}^{(\mathrm{D})},S)u_i[s] \ .$$

$\nu_{\max}^{(\mathrm{D})}$ is the normalized Doppler bandwidth, and $S_{\mathrm{D}} \le I \le S$ with $S_{\mathrm{D}} = \left\lceil 2\nu_{\max}^{(\mathrm{D})}S \right\rceil + 1$ representing the approximate signal space dimension. The reduction of the space dimension, due to eigenvalues $\lambda_i(\nu_{\max}^{(\mathrm{D})},S)$ rapidly becoming negligible for $i > 2\nu_{\max}^{(\mathrm{D})}S$, means less coefficients to be estimated. Furthermore, no assumption on the stochastic model for the channel is needed except knowledge of the maximum Doppler spread. Channel estimation is evaluated via relative MMSE

$$\delta_H = \frac{\mathbb{E}\{|H_{n,k}[m,s] - \hat{H}_{n,k}[m,s]|^2\}}{\mathbb{E}\{|H_{n,k}[m,s]|^2\}} \ .$$

From (1) and (3), denoting $\boldsymbol{u}[s] = (u_1[s],\ldots,u_I[s])^{\mathrm{T}}$, $\boldsymbol{\xi}[m,s] = \boldsymbol{x}[m,s] \otimes \boldsymbol{u}[s]$, $\boldsymbol{\Xi}[m,s] = \boldsymbol{I}_N \otimes \boldsymbol{\xi}^{\mathrm{T}}[m,s]$, $\boldsymbol{\psi}_{n,k}[m] = (\psi_{n,k}[m,1],\ldots,\psi_{n,k}[m,I])^{\mathrm{T}}$, $\boldsymbol{\psi}_n[m] = \left(\boldsymbol{\psi}_{n,1}^{\mathrm{T}}[m],\ldots,\boldsymbol{\psi}_{n,K}^{\mathrm{T}}[m]\right)^{\mathrm{T}}$, $\boldsymbol{\psi}[m] = \left(\boldsymbol{\psi}_1^{\mathrm{T}}[m],\ldots,\boldsymbol{\psi}_N^{\mathrm{T}}[m]\right)^{\mathrm{T}}$, we get $\boldsymbol{r}[m,s] = \boldsymbol{\Xi}[m,s]\boldsymbol{\psi}[m] + \boldsymbol{w}[m,s]$, and finally, collecting all the OFDM received symbols and denoting $\boldsymbol{r}[m] = \left(\boldsymbol{r}^{\mathrm{T}}[m,1],\ldots,\boldsymbol{r}^{\mathrm{T}}[m,S]\right)^{\mathrm{T}}$, $\boldsymbol{\Xi}[m] = \left(\boldsymbol{\Xi}^{\mathrm{T}}[m,1],\ldots,\boldsymbol{\Xi}^{\mathrm{T}}[m,S]\right)^{\mathrm{T}}$, $\boldsymbol{w}[m] = \left(\boldsymbol{w}^{\mathrm{T}}[m,1],\ldots,\boldsymbol{w}^{\mathrm{T}}[m,S]\right)^{\mathrm{T}}$, we obtain the signal model for the channel estimation as

$$\boldsymbol{r}[m] = \boldsymbol{\Xi}[m]\boldsymbol{\psi}[m] + \boldsymbol{w}[m] \ . \tag{4}$$

We omit the index m to simplify notation. Confining to linear channel estimators, i.e. $\hat{\boldsymbol{\psi}} = \boldsymbol{A}_\psi \boldsymbol{r}$, where is given by $\boldsymbol{A}_\psi = \arg\min_{\boldsymbol{A}} \mathbb{E}\left\{|\boldsymbol{\psi} - \boldsymbol{A}\boldsymbol{r}|^2\right\} = \mathbb{E}\left\{\boldsymbol{\psi}\boldsymbol{r}^{\mathrm{H}}\right\}\left(\mathbb{E}\left\{\boldsymbol{r}\boldsymbol{r}^{\mathrm{H}}\right\}\right)^{-1}$. From (4) we have

$$\begin{aligned} \mathbb{E}\left\{\boldsymbol{r}\boldsymbol{r}^{\mathrm{H}}\right\} &= \mathbb{E}\left\{\boldsymbol{\Xi}\boldsymbol{C}_\psi\boldsymbol{\Xi}^{\mathrm{H}}\right\} + \sigma_w^2\boldsymbol{I}_{SN} \ , \\ \mathbb{E}\left\{\boldsymbol{\psi}\boldsymbol{r}^{\mathrm{H}}\right\} &= \boldsymbol{C}_\psi\hat{\boldsymbol{\Xi}}^{\mathrm{H}} \ , \end{aligned}$$

being $\boldsymbol{C}_\psi = \mathbb{E}\left\{\boldsymbol{\psi}\boldsymbol{\psi}^{\mathrm{H}}\right\} = \frac{1}{2\nu_{\max}^{(\mathrm{D})}}\mathrm{diag}\left(\boldsymbol{\lambda}_\psi\right)$, $\boldsymbol{\lambda}_\psi = \boldsymbol{e}_{NK} \otimes \boldsymbol{\lambda}$, $\boldsymbol{\lambda} = (\lambda_1,\ldots,\lambda_I)^{\mathrm{T}}$, and $\hat{\boldsymbol{\Xi}} = \mathbb{E}\{\boldsymbol{\Xi}\}$. The diagonal structure of $\boldsymbol{C}_\psi$ is due to the independence of channels among different transmit antennas and/or receive antennas, and to the orthogonality of the discrete prolate spheroidal sequences, i.e.

$$\mathbb{E}\left\{\psi_{n,k}[m,i]\psi_{n',k'}^*[m,j]\right\} = \frac{\lambda_i}{2\nu_{\max}^{(\mathrm{D})}}\delta_{n,n'}\delta_{k,k'}\delta_{i,j} \ .$$

The independence of transmit antennas and also of OFDM symbols (due to the effect of random interleaving), i.e $\mathbb{E}\left\{x_k[m,s]x_{k'}^*[m,s']\right\} = \begin{cases} 1 & k=k', s=s' \\ \hat{x}_k[m,s]\hat{x}_{k'}^*[m,s'] & \text{else} \end{cases}$ gives $\mathbb{E}\left\{\boldsymbol{\Xi}\boldsymbol{C}_\psi\boldsymbol{\Xi}^{\mathrm{H}}\right\} = \begin{pmatrix} \boldsymbol{\Phi}_{1,1} & \ldots & \boldsymbol{\Phi}_{1,S} \\ \vdots & \ddots & \vdots \\ \boldsymbol{\Phi}_{S,1} & \ldots & \boldsymbol{\Phi}_{S,S} \end{pmatrix}$, with $\boldsymbol{\Phi}_{s,s'} = \mathrm{diag}(\phi_{s,s'}\boldsymbol{e}_N)$, and with

$$\phi_{s,s'} = \begin{cases} \sum_{i=1}^{I}\sum_{k=1}^{K} \frac{\lambda_i}{2\nu_{\max}^{(\mathrm{D})}}|u_i[s]|^2 & s = s' \\ \sum_{i=1}^{I}\sum_{k=1}^{K} \frac{\lambda_i}{2\nu_{\max}^{(\mathrm{D})}}u_i[s]u_i^*[s']\hat{x}_k[m,s]\hat{x}_k^*[m,s'] & \text{else} \end{cases}$$

It is then straightforward to obtain $\mathbb{E}\left\{\boldsymbol{\Xi}\boldsymbol{C}_\psi\boldsymbol{\Xi}^{\mathrm{H}}\right\} = \hat{\boldsymbol{\Xi}}\boldsymbol{C}_\psi\hat{\boldsymbol{\Xi}}^{\mathrm{H}} + \boldsymbol{\Theta}$, being $\boldsymbol{\Theta} = \mathrm{diag}(\boldsymbol{\vartheta} \otimes \boldsymbol{e}_N)$, $\boldsymbol{\vartheta} = (\vartheta_1,\ldots,\vartheta_S)^{\mathrm{T}}$, and $\vartheta_s = \sum_{i=1}^{I}\sum_{k=1}^{K} \frac{\lambda_i}{2\nu_{\max}^{(\mathrm{D})}}|u_i[s]|^2\left(1 - |\hat{x}_k[m,s]|^2\right)$, and finally

$$\boldsymbol{A}_\psi = \boldsymbol{C}_\psi\hat{\boldsymbol{\Xi}}^{\mathrm{H}}\left(\hat{\boldsymbol{\Xi}}\boldsymbol{C}_\psi\hat{\boldsymbol{\Xi}}^{\mathrm{H}} + \boldsymbol{\Delta}\right)^{-1} \ ,$$

with $\boldsymbol{\Delta} = \boldsymbol{\Theta} + \sigma_w^2\boldsymbol{I}_{SN}$. The channel estimate is obtained as

$$\hat{\boldsymbol{\psi}} = \left(\hat{\boldsymbol{\Xi}}^{\mathrm{H}}\boldsymbol{\Delta}^{-1}\hat{\boldsymbol{\Xi}} + \boldsymbol{C}_\psi^{-1}\right)^{-1}\hat{\boldsymbol{\Xi}}^{\mathrm{H}}\boldsymbol{\Delta}^{-1}\boldsymbol{r} \ , \tag{5}$$

to be used in (3). Eq. (5), by using the matrix inversion lemma, replaces the inversion of a $SN \times SN$ matrix with the inversion of a $NKI \times NKI$ matrix, saving computations when $K < 1/(2\nu_{\max}^{(\mathrm{D})})$. Also it is worth noticing that $\boldsymbol{\Delta}$ is diagonal, thus its inversion is not computationally prohibitive.

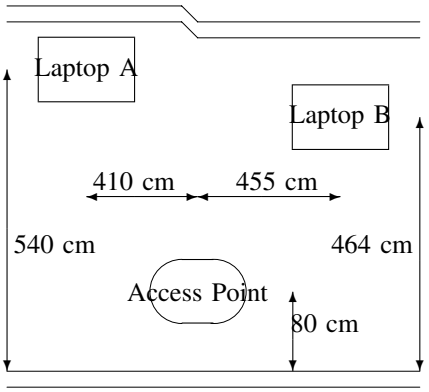

Fig. 1. Equipment positions.

IV. Real-Channel Measurements

The performance of the developed detector/estimators will be studied for the real measured MIMO channel from the initial measurement campaign at Lund University, Sweden, in November 2006 within the WILATI project. The measurement setup and parameters are summarized in the following.

The sounded MIMO channel corresponds to one receiver with 8 antenna elements and two transmitters each with 4 antenna elements, one considered as the desired user and one as the interferer. The receiver is a uniform circular array with 8 vertical polarized patch elements, referred as Access Point in Fig. 1. The two transmitters are two laptops each equipped with 4 antenna elements mounted on the sides of the screen. The RUSK channel sounder is employed to measure the channel impulse response (both laptops are connected to the transmitter side of the RUSK channel sounder) [14], [18]. In Fig. 1 the distances between the equipments are depicted.

The measurements are done for three different scenario as follows: (i) when the environment is quiet (stationary); (ii) when the laptop is moving and the environment is quiet (moving laptop); (iii) when people are moving around (dynamic). Sec. V shows results referring to the dynamic scenario.

The RUSK channel sounder applies correlation technique. A periodic muti-tone broadband test sequence is generated at the transmitter. This signal is distributed to the transmit antennas by fast multiplexing and then excites the radio channel. At the receiver also fast multiplexing is used. The arriving signal is correlated with a local copy of the test sequence and then the channel impulse response is extracted for each pair of transmit and receive antenna elements and stored as vector channel impulse snapshots [14], [18].

Tab. I reports the measured parameters. The resulting data files from the measurements include two 4×8 MIMO channels for the three mentioned scenarios, which will be used to test the performance of the proposed estimator/detector.

V. Results

Numerical performance in terms of BER-vs-SNR and relative MSSE-vs-SNR have been obtained for various systems, and compared with the Single-User Bound (SUB) performance. SUB, used as a reference, represents the performance achieved by a system with a single transmit antenna and perfect knowledge of channel coefficients at the receiver.

TABLE I

Measurement parameters.

Center frequency	5.2 GHz
Bandwidth	240 MHz
Test signal length	3.2 s
TX power	0.5 W (27 dBm)
Number of measured blocks	200
Gap between blocks	1.4 ms

Results shown here refer to systems with $M = 32$ subcarriers and $S = 128$ OFDM symbols per frame thus corresponding to $L = 4,096$ code bits per frame. In each frame we used $S_p = 24$ (resp. $S_p = 12$) pilot OFDM symbols, i.e. $\approx 20\%$ (resp. $\approx 10\%$). Excluding pilots we have $3,328$ (resp. $3,712$)code bits generated at rate $R = 1/2$ via a recursive systematic convolutional encoder [10] with generators $(7,5)_8$ and with two tail bits used to enforce the final state into 1, thus $L_b = 1,662$ (resp. $1,854$) source bits per OFDM block. Channel coefficients have been obtained from the dynamic scenario described in Sec. IV. For channel estimation $\nu_{\max}^{(\mathrm{D})} = 0.005$ has been assumed, the signal space dimension is reduced from $S = 128$ to $S_{\mathrm{D}} = 2$, and we used $I = 5$ coefficients for series expansion. We averaged over 500 different choices of transmit/receive antennas.

Fig. 2 refer to a system with $N = 2$ receive antennas, $K = 2$ transmit antennas (both 20% and 10% of pilots overhead), while Fig. 3to a system with $N = 4$ receive antennas, $K = 4$ transmit antennas (only 10% of pilots overhead). They show how after a few iterations the receiver approaches convergence both for BER and relative MMSE. The loss for reducing pilots overhead from 20% to 10% is quite negligible, expecially for SNR large than 10 dB. Comparison with SUB performance show a 2dB (resp. 6 dB) loss in the case of a 2×2 (4×4) system. We believe this is due to the presence of frequency correlation in the channel that is not exploited at the receiver, meaning that performance that a user would experience can be further improved takinf into account frequency correlation in the channel estimation process.

VI. Conclusions

This paper described an iterative receiver for joint channel estimation and multiuser detection, and tests on real measurements from indoor scenario. The performance showed a loss with respect to SUB, meaning that exploiting appropriately frequency correlation (here neglected) gives chances for further improvements. We are currently working to modify the channel estimator in order to exploit frequency correlation, and fill the gap between experienced performance and SUB.

Acknowledgment

The authors would like to thank Peter Almers and Fredrick Tufvesson at Lund University, Sweden, for providing the measurements data.

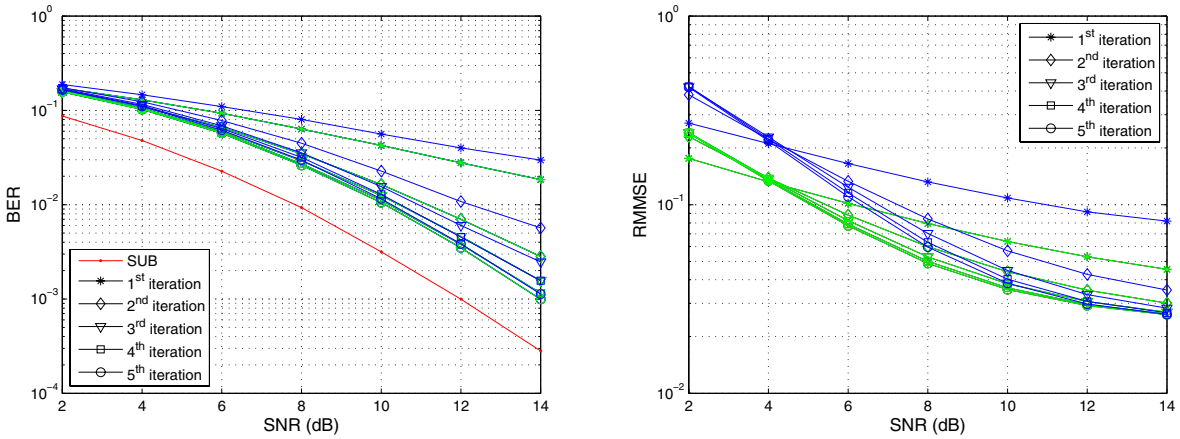

Fig. 2. BER and relative MMSE vs SNR. 2×2 systems with 20% (green curves) and 10% (blue curves) of pilot overhead.

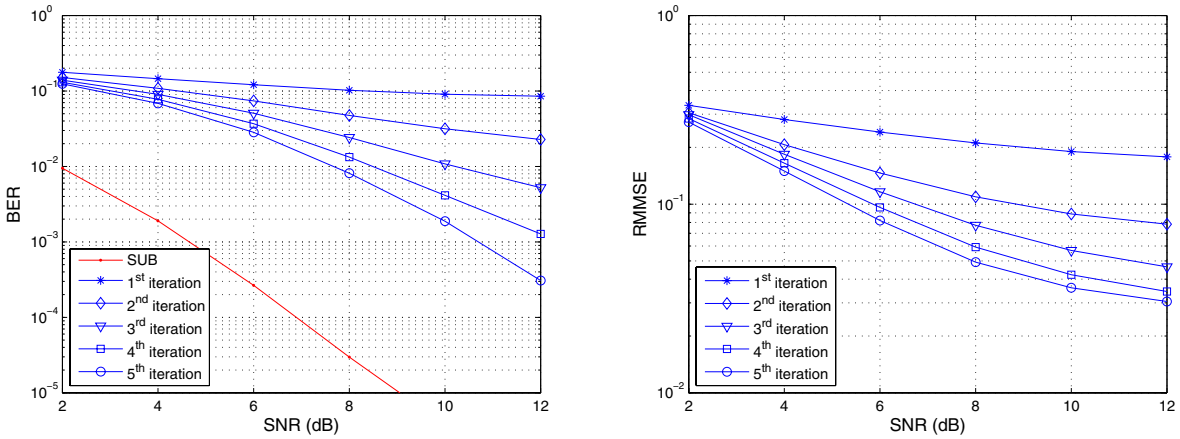

Fig. 3. BER and relative MMSE vs SNR. 4×4 systems with 10% of pilot overhead.

REFERENCES

[1] P. Almers, J. Koivunen, V.M. Kolmonen, "Report on Environment Selection for Measurement Campaign, and Literature Study for (Non-Interference) Propagation Measurements," D1.1, WILATI project, NORDITE Technology Program 2006.

[2] L.R. Bahl, J. Cocke, F. Jelinek, J. Raviv, "Optimal Decoding of Linear Codes for Minimizing Symbol Error Rate," *IEEE Trans. Inf. Theory*, vol. 20(2), pp. 284-287, Mar. 1974.

[3] J. Boutros, G. Caire, "Iterative Multiuser Joint Decoding: Unified Framework and Asymptotic Analysis," *IEEE Trans. Inf. Theory*, vol. 48(7), pp. 1772-1793, Jul. 2002.

[4] A. Goldsmith, *Wireless Communications*, Cambridge Univ. Press, 2005.

[5] T.S. John, A. Nallanathan, M.A. Armand, "A Pilot-Aided Non-Resampling Sequential Monte Carlo Detector for Coded MIMO-Systems," *IEEE GLOBECOM*, vol. 4, pp. 2250-2254, Nov./Dec. 2005.

[6] Y. Li, J.H. Winters, N.R. Sollenberger, "MIMO-OFDM for Wireless Communications: Signal Detection with Enhanced Channel Estimation," *IEEE Trans. Comm.*, vol. 50(9), pp. 1471-1477, Sep. 2002.

[7] D.N. Liu, M.P. Fits, "Low Complexity Affine MMSE Detector for Iterative Detection-Decoding MIMO OFDM Systems," *IEEE ICC*, vol. 10, pp. 4654-4659, Jun. 2006.

[8] M. Lončar, R.R. Müller, J. Wehinger, C.F. Mecklenbräuer, T. Abe, "Iterative Channel Estimation and Data Detection in Frequency-Selective Fading MIMO Channels," *European Trans. Telecomm.*, vol. 15(5), pp. 459-470, Sep./Oct. 2004.

[9] B. Lu, G. Yue, X. Wang, "Performance Analysis and Design Optimization of LPDC-Coded MIMO OFDM Systems," *IEEE Trans. Sig. Processing*, vol. 52(2), pp. 348-361, Feb. 2004.

[10] J.G. Proakis, *Digital Communications*, McGraw Hill, 2000.

[11] P. Robertson, E. Villebrun, E. Höher, "A Comparison of Optimal and Sub-Optimal MAP Decoding Algorithms Operating in the Log Domain," *IEEE ICC*, vol. 2, pp. 1009-1013, Jun. 1995.

[12] P. Salvo Rossi, R.R. Müller, "Joint Iterative Time-Variant Channel Estimation and Multi-User Detection for MIMO-OFDM Systems," *IEEE GLOBECOM*, Nov. 2007, accepted for publication.

[13] G.L. Stüber, J.R. Barry, S.W. McLaughlin, Y. Li, M.A. Ingram, T.G. Pratt, "Broadband MIMO-OFDM for Wireless Comm.," *Procs. of the IEEE*, vol. 92(2), pp. 271-294, Feb. 2004.

[14] U. Tratwein and D. Brueckner, "Channel Sounding with RUSK: A Tutorial," ©2002–2005 MEDAV GmbH. `http://www.medav.de`

[15] S. Verdú, *Multiuser Detection*, Cambridge Univ. Press, 1998.

[16] X. Wang, H.V. Poor, "Iterative (Turbo) Soft Interference Cancellation and Decoding for Coded CDMA," *IEEE Trans. Comm.*, vol. 47(7), pp. 1046-1061, Jul. 1999.

[17] T. Zemen, C.F. Mecklenbräuer, J. Wehinger, R.R. Müller, "Iterative Joint Time-Variant Channel Estimation and Multi-User Detection for MC-CDMA," *IEEE Trans. Wireless Comm.*, vol. 5(6), pp. 1469-1478, Jun. 2006.

[18] "RUSK-MIMO Product information," MEDAV GMbH 2001.